ELECTRONIC SUPPORTING INFORMATION

Yiming Yin[a,b], Alexander S. Goloveshkin[c], Dmitrii Kopytov[d], Anastasiya Parashuk[d], Egor Latipov[e], Guo Zhipeng[a,b], Ivan Khanbekov[d], Yanan Zhu[b], Valentina V. Utochnikova[a,f]

[a] Faculty of Materials Science, M. V. Lomonosov Moscow State University, 1/3 Leninskye Gory, Moscow, 119991, Russia.

[b] Faculty of Materials Science, Shenzhen MSU-BIT University, Shenzhen, 518172, P. R. China.

[c] Nesmeyanov Institute of Organoelement Compounds of Russian Academy of Sciences, Moscow 119934, Russian Federation

[d] Chimmed Group, 3 Kashirskoe shosse, 2, 4/9, Moscow, 115230, Russia

[e] Institute of Nanotechnology of Microelectronics of the Russian Academy of Sciences, Leninsky Prospect 32A, Moscow, 119334, Russia

[f] School of Chemical Engineering and Technology, Tianjin University, Tianjin, 300354, China

[g] Moscow Institute of Physics and Technology, 9, Institutsky Ln., Dolgoprudny, 141701, Russian Federation

Contents

1. Materials and Synthesis details

All reagents and chemicals were purchased from commercial sources and used without additional purification. The following reagents were used as starting reagents: 1,10-phenanthroline (phen, >99%), $EuCl_3 \cdot 6H_2O$ (99%), benzenetricarboxylic acid (H_3btc, 99%), benzenetetracarboxylic acid (H_4btec, 99%).

Compounds **I, II** were synthesized *via* solution synthsis. To obtain the **Eu(btc)(Phen)(H_2O)$_2$** (Compound **I**), H_3btc (0.35 mmol) was dissolved in aqueous solution (25 ml) of 0.9 mmol of KOH, then filtered from the excess of H_3btc, and the filtrate was added to the water solution of 0.3 mmol of the lanthanide nitrate $EuCl_3 \cdot 6H_2O$. The precipitate was immediately formed, stirred for 6 h, then filtered off and washed three times with distilled water, and dried to obtain the white powder. Similarly, **K[Eu(btec)(Phen)](H_2O)$_2$** (Compound **II**) was obtained by dissolving H_4btec (0.35 mmol) in aqueous solution (25 ml) of 1.2 mmol of KOH, which was then filtered from the excess of H_4btc, and the filtrate was added to the water solution of 0.3 mmol of the lanthanide nitrate $EuCl_3 \cdot 6H_2O$. The immediately formed precipitate was stirred for 6 h, filtered off, washed three times with distilled water, and dried to obtain the white powder.

2. Analysis methods, equipment and technical details of experiments

The IR spectra of the compounds were recorded using a Perkin Elmer SpectrumOne FTIR spectrometer in the range 350-7800 cm^{-1}. **Thermal analysis (TA)** was performed on a NETZSCH STA 409 PC Luxx thermal analyzer (NETZSCH, Germany) at a heating rate of 10 °C/min (sample weight 5-10 mg). The composition of the gas phase formed during decomposition of the samples was studied using a quadrupole mass spectrometer QMS 403C Aeolos (NETZSCH, Germany) combined with a thermal analyzer NETZSCH STA 409 PC Luxx. Mass spectra were recorded for the mass numbers 18 (H_2O), 44 (CO_2) and 58 (acetone). **Powder diffraction (PXRD)** was measured using a Bruker D8 Advance Vario diffractometer with Ge(111) using a monochromator in the transmission mode between polyester films (Mylar), as well as on a Bruker D8 Advance diffractometer in reflection mode using a silicon stand (Bragg-Brentano geometry, with variable slits). Both diffractometers are equipped with a LynxEye 1D detector.

Photoluminescence spectra and excitation spectra were measured on a Fluoromax spectrofluorometer using a xenon lamp with tunable wavelength as an excitation source. All luminescence and excitation spectra were removed with an adjustment for instrumental functions. The excitation spectra were recorded at a wavelength of 612 nm. The lifetime of the excited state was determined using a Fluoromax spectrofluorometer. This value is a luminescent characteristic sensitive to the coordination environment and is determined from the luminescence attenuation curves according to equation :

$$y=y_o+B\ exp\left(-\frac{t}{\tau}\right)$$

where y is the measured luminescence intensity at time t after the laser pulse, B is the luminescence intensity at time t=0, $\tau=\tau_{obs}$ is the lifetime of the excited state, or the decay time of luminescence, y_0 is the consideration of the background signal. The quantum yields of the powders were measured at room temperature when excited through a ligand to characterize the luminescence efficiency. Measurements were performed on a Fluoromax spectrofluorometer using an integrating sphere.

Cathodoluminescence spectra were measured by the special self-made setup (Figure S1), which made by ourselves.It consists of an analytical vacuum chamber (1) connected to an oil-free pumping system (2). On the chamber, there is a high-voltage vacuum-tight electrical input for connecting the substrate holder traverse (3) located on the loading flange (4), a wide-range vacuum sensor (5), a quadrupole mass spectrometer (6), an electronic beam gun (7), gas leak (8), quartz tube (9), quartz exit window (10), high-vacuum slide gate (11). The head of the optical radiation power meter or the waveguide of the optical spectrometer is connected to the output quartz window (10).

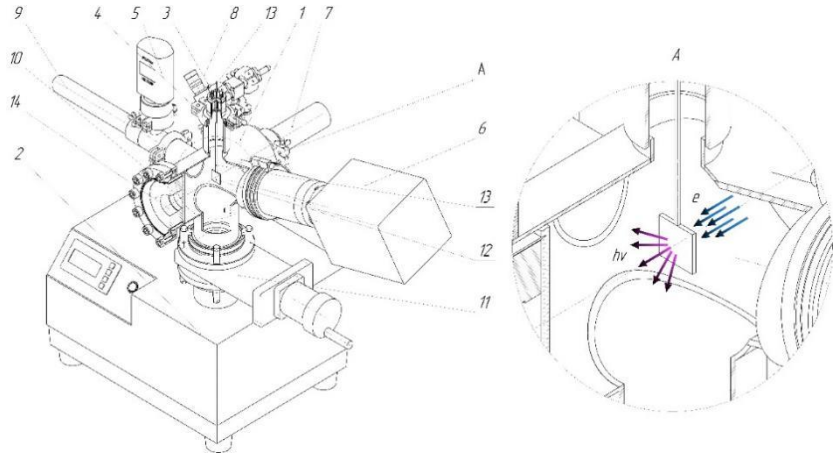

Figure S1. Laboratory vacuum installation for determining the output characteristics of cathodoluminophores.

The system is pumped out by a pre-vacuum pump to a pressure not higher than $1 \cdot 10^{-2}$ Torr, then a high-vacuum turbomolecular pump is turned on and pumped out to a pressure not higher than $5 \cdot 10^{-7}$ Torr. The operating temperature W of the cathode is in the range of 2400-2600 °C, and the efficiency of the cathode is 2-10 mA/W. The optical head is installed in the seat (14) of the output quartz window (10). The power of optical radiation is measured in W/m^2.

X-ray excited luminescence was recorded by Optosky ATP-2000. The experimental studies were performed using a Microfocus X-ray computed tomograph PRDU, mass-produced by Eltechmed (St. Petersburg, Russia) (Figure S2). The tomography system comprises an X-ray protection chamber, a precision object manipulation stage, a flat-panel digital detector, a microfocus X-ray source, and integrated control and data processing software. The microfocus X-ray tube operates at voltages ranging from 40 to 90 kV and currents from 10 to 80 μA, with a maximum continuous power of 8 W. The source provides high spatial resolution due to a focal spot size of 5 μm. The tube is equipped with a 0.2 mm Beryllium filter and features a target angle of 20° and a beam geometry of 40°. The X-ray detector features a sensitive area of 145×228 mm with a pixel size of ⩽50 μm and a 14-bit ADC, providing high-contrast imaging capabilities.

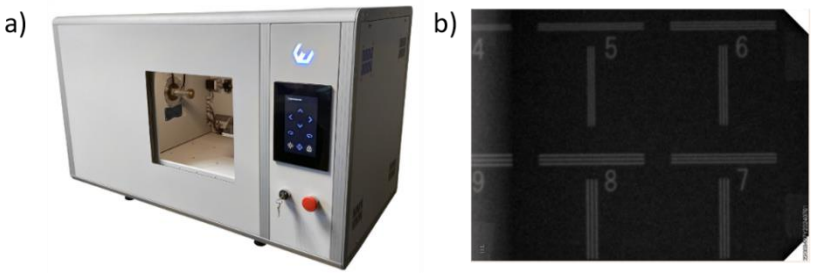

Figure S2. a) Microfocus X-ray computed tomograph PRDU Eltechmed. b) Jima test 5 μm X-Ray Tube

The X-ray tube (prototype unit developed by NPO *Vacuum Technologies*) was mounted on a laboratory bench, with the operator's position located laterally outside the direct radiation field (Figure S1). Dosimetric monitoring was carried out using a **Polimaster PM1621A** dosimeter (primary reference), two **ID-02** direct-reading dosimeters, and a **RadiaCode-110** spectrometric dosimeter. The PM1621A was positioned at 57 cm from the X-ray window, which was taken as the reference distance for dose rate measurements. The ID-02 units were worn on the operator's chest, and the RadiaCode-110 was placed on the bench for independent monitoring of exposure levels.

Figure S3. Photograph of the test setup

3. Characterization of the X-ray source

3.1 Measurement protocol.

Tube operation parameters (voltage 60–90 kV, current 10–90 μA) were set using dedicated PC software. Exposure time was controlled by an external stopwatch, with individual runs not exceeding 90 s. For each measurement, the ambient dose equivalent rate H*(10) was recorded in units of mSv h^{-1}, and cumulative dose in mrem was logged. Where required, dose rates were recalculated to alternative distances (20 mm and 100 mm) using the inverse square law.

Table S1: full list of recorded measurement parameters (U, I, D, dose rate, cumulative dose, recalculated values at 20 mm and 100 mm).

Measurement №	Device	U, kV	I, μA	D, cm	MD, mSv/h	t, s	D, mrem	MD, Sv/h at 20mm	MD, Sv/h at 100mm
1	PM1621A	60	10	57	38			30.9	1.2
2	PM1621A	60	30	57	102			82.8	3.3
3	PM1621A	60	90	57	4.6			3.7	0.1
4	PM1621A	60	60	57	202			164.1	6.6
5	PM1621A	60	80	57	--				
6	PM1621A	60	70	57	--				
7	PM1621A	70	10	57	38.8			31.5	1.3
8	PM1621A	80	10	57	11.4			9.3	0.4
9	PM1621A	60	60	57	223			181.1	7.2
10	PM1621A	90	10	57	66.6			54.1	2.2
11	PM1621A	80	10	57	9.23			7.5	0.3
12	PM1621A	80	30	57	158			128.3	5.1
13	PM1621A	80	60	57	333			270.5	10.8
14	PM1621A	80	90	57	535			434.6	17.4
15	PM1621A	90	30	57	177			143.8	5.8

16	Id02 1	60	10	57	15	60	25	12.2	0.5
17	Id02 2	60	10	57	18	60	30	14.6	0.6
18	Id02 1	90	10	57	28.8	60	48	23.4	0.9
19	Id02 2	90	10	57	33	60	55	26.8	1.1
20	Id02 1	90	30	57	67.2	60	112	54.6	2.2
21	Id02 2	90	30	57	72	60	120	58.5	2.3

3.2 Safety monitoring

During the entire testing campaign (21 runs, total duration ~2 h), the accumulated operator dose remained < 2 mrem, well within non-occupational exposure limits. The maximum recorded dose rate at the operator's position was 0.3 mSv h^{-1}, while the ambient background level was ~0.1 μSv h^{-1}. For remote observation, a smartphone camera linked to an external display was used to read instrument data without direct exposure.

3.3 Results

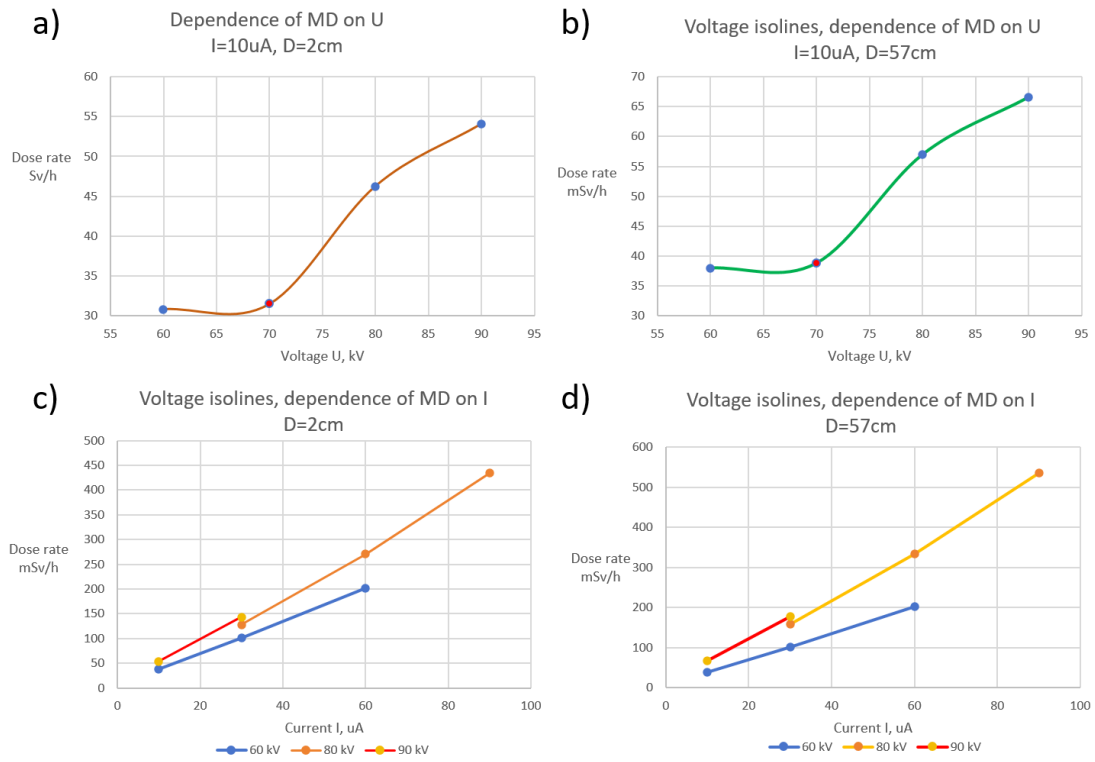

Figure S4: Isodose contour maps and voltage/current dependencies obtained from Excel analysis.

- At 57 cm, measured H*(10) ranged from **38 mSv h⁻¹** (60 kV, 10 µA) to **535 mSv h⁻¹** (80 kV, 90 µA).
- Recalculated values at 20 mm correspond to **30.9–434.6 Sv h⁻¹**, confirming sufficient photon flux for luminescence excitation.
- Dose rate scaled linearly with tube current, whereas the dependence on acceleration voltage was less systematic.
- Instabilities were observed at high loads (≥ 70 µA at 60 kV or ≥ 10 µA at 80–90 kV), where automatic shutdown or reduced dose rates occurred.
- Startup delay was consistently noted: emission intensity required several seconds to stabilize after switching on.

3.4 Validation.

Measurements with ID-02 dosimeters yielded dose rates 2–2.5× lower than PM1621A, consistent with their energy calibration differences. RadiaCode-110 confirmed the onset of X-ray emission but did not provide reliable spectral data at close distances due to count rate saturation.

3.5 Summary

The prototype X-ray source delivered stable radiation output in the 60–90 kV, 10–90 μA operating range, with linear current scaling and maximum dose rates suitable for excitation of thin-film luminescent materials. Identified limitations included occasional automatic shutdown at high load, delayed stabilization after switching, and insufficient shielding for safe routine operation.

4. Compounds characterization

4.1 PXRD data

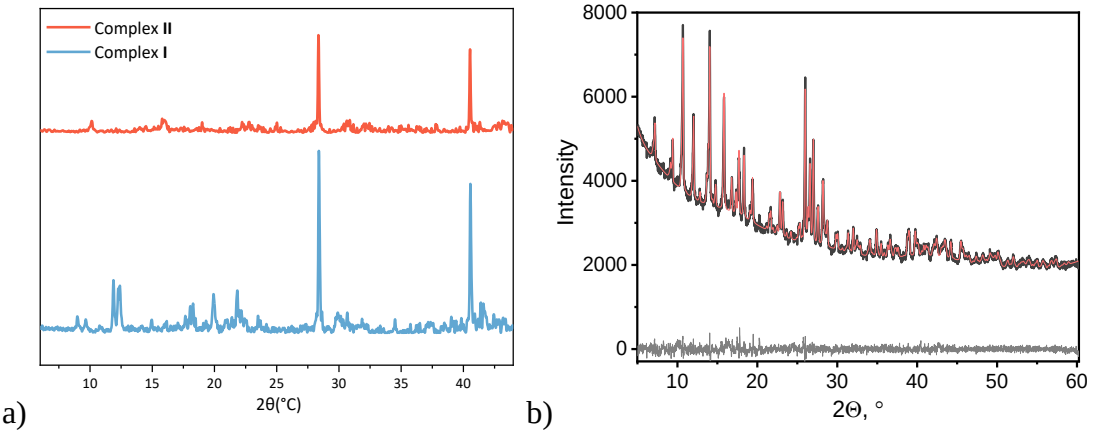

Figure S5. The PXRD patterns of compounds a**) I and II** and b) **II**: experiment (black), calculated (red), and difference (grey)

Table S2. Indexing data of **I** = $[KEu(btec)phen(H_2O)_2]_n$ and **II** = $[Eu(btc)phen(H_2O)_2]_n$

Parameter	**I**	**II**
R-Bragg	0.035	0.053
Spacegroup	Pbca	$P2_12_12_1$
Cell Volume (Å^3)	4262.0(8)	2094.4(3)
a (Å)	19.714(2)	19.301(2)
b (Å)	14.9311(17)	15.8611(18)
c (Å)	14.4790(16)	6.8416(4)

4.2. TGA data

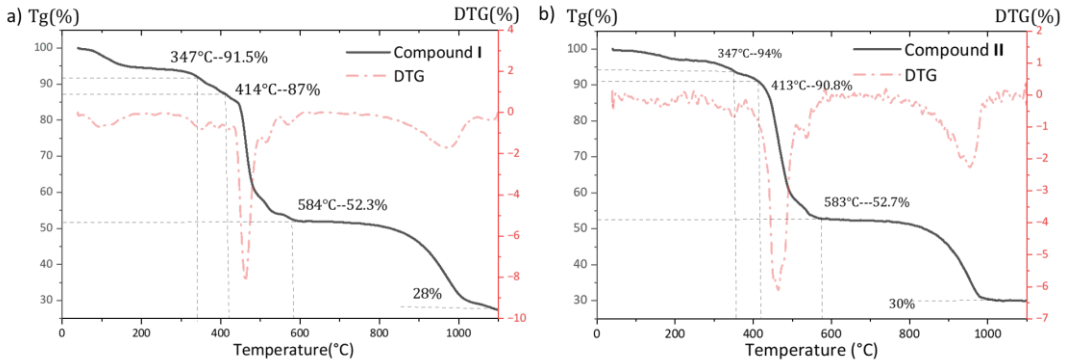

Figure S6. The TGA of a) compound **I,** b) compound **II**

Table S3. The data TGA of $[KEu(btec)phen(H_2O)_2]_n$ and $[Eu(btc)phen(H_2O)_2]_n$

Temperature range	Reaction	m(residue), found%	m(residue), clcd%
	$[Eu(btec)(phen)(H_2O)_2]$		
40-347°C	- H_2O	91.5	93.7
347-583°C	- Phen	75.0	62.4
413-583°C	- btec	52.3	42.1
	→$Eu_2(CO_3)_3$		
583-1000°C	→ Eu_2O_3	28	30.6
	$[KEu(btc)(phen)(H_2O)_2]$		
40-347°C	- H_2O	94	94.5
347-583°C	- Phen	83	67.2
413-583°C	- btec	52.7	36.7
	→$Eu_2(CO_3)_3$/ K_2CO_3		
583-1000°C	→ Eu_2O_3 / K_2O_2/ KO_2/K_2CO_3	30	26.7

4.3 Vibrational spectroscopy

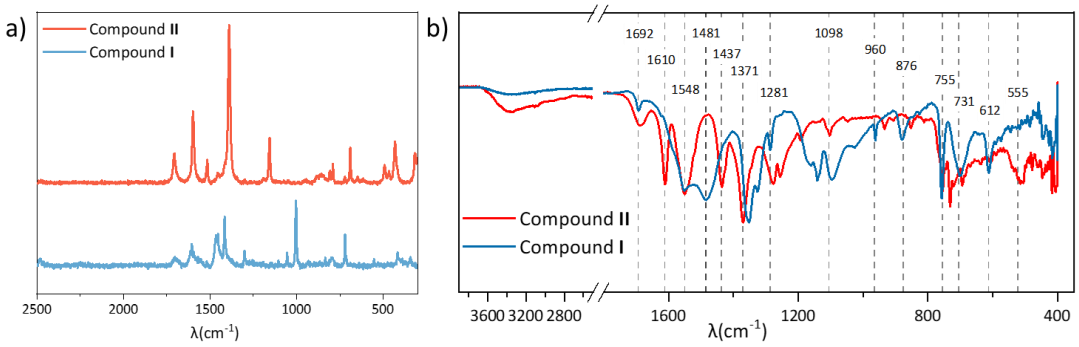

Figure S7. a) The Raman spectra under 785 nm laser, and b) IR spectra of **I** and **II**

4.4 Photoluminescence

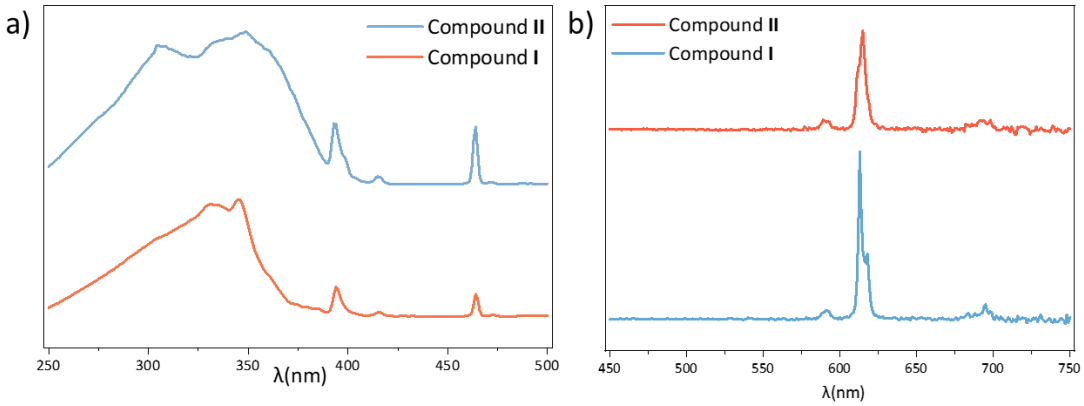

Figure S8. The photoluminescence spectra of **I and II**: a) excitation λ_{em}=613 nm, b) emission λ_{ex} = 350 nm spectra

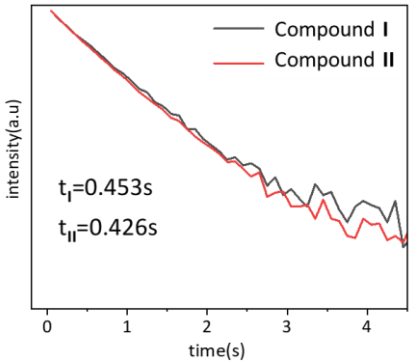

Figure S9. The lifetime of compound (**I-II**)

4.5 Cathodoluminescence

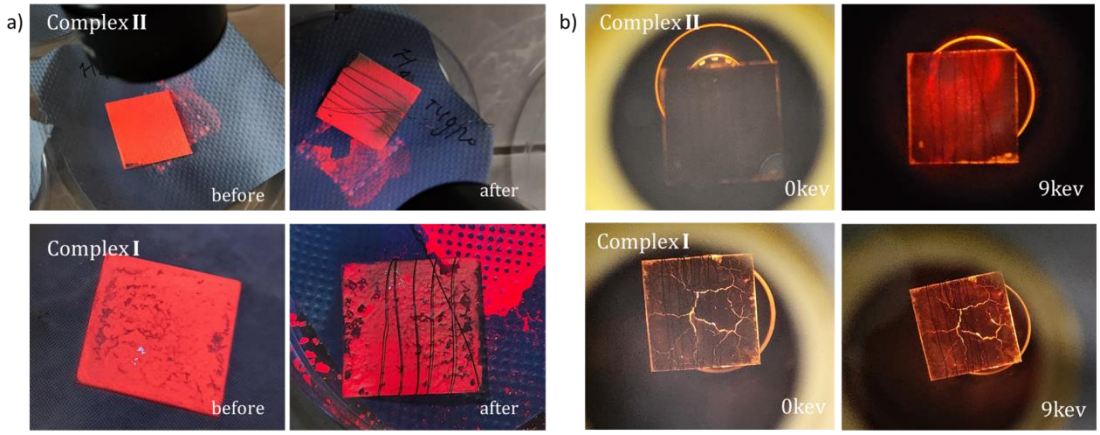

Figure S10. a) Photoluminescence images before and after measurement cathodoluminescence under 254 nm UV light illumination, and b) Cathodoluminescence images of films under 0 and 9 keV of films of compound (**I-II**).

4.6 X-ray excited luminescence

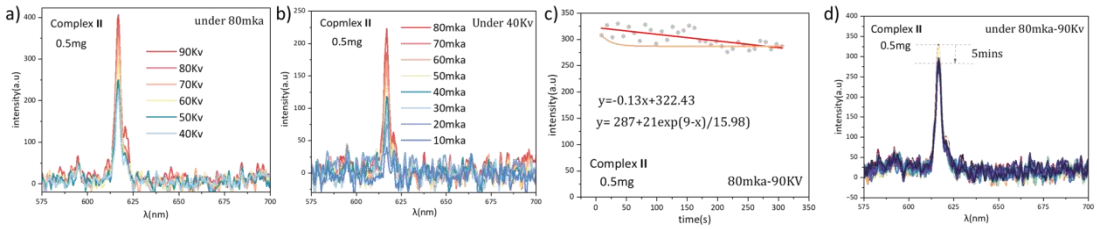

Figure S11. The X-ray luminescence (RL) spectrum of compound **II** a) from 40 to 90kV under 80μA, b) from 10 to 100μA under 40kV, and c,d) time decay (5mins) of intensity RL under 80μA and 90kV.

Table S4. The equation of X-ray excited luminescence intensity of Compound II

	Quality	I_{max}	Function time decay
Compound **I**	1mg	1300	$y=1294+24e^{((16-x)/91)}$
Compound **II**	0.5mg	400	$y= 287+21e^{(9-x)/15.98)}$
Compound **II**	0.5mg	1700	$y=1317+408e^{(-21.8-x)/282.79)}$
Compound **II**	1mg	3100	$y=2462.62+570.83e^{(43.36-x)/267.55)}$